Identification of Novel Amino Acid Derived CCK-2R Antagonists As Potential Antiulcer Agent: Homology Modeling, Design, Synthesis, and Pharmacology

ARTICLE *in* JOURNAL OF CHEMICAL INFORMATION AND MODELING · JANUARY 2013

Impact Factor: 3.74 · DOI: 10.1021/ci3003655

7 AUTHORS, INCLUDING:

Amit K Gupta
University of Texas Health Science Center at H…
14 PUBLICATIONS **68** CITATIONS
SEE PROFILE

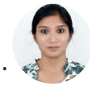

Kanika Varshney
Central Drug Research Institute
5 PUBLICATIONS **27** CITATIONS
SEE PROFILE

Vaibhav Mishra
Central Drug Research Institute
15 PUBLICATIONS **80** CITATIONS
SEE PROFILE

Gautam Palit
Central Drug Research Institute
93 PUBLICATIONS **1,199** CITATIONS
SEE PROFILE

JOURNAL OF CHEMICAL INFORMATION AND MODELING

Article

pubs.acs.org/jcim

Identification of Novel Amino Acid Derived CCK-2R Antagonists As Potential Antiulcer Agent: Homology Modeling, Design, Synthesis, and Pharmacology

Amit K. Gupta,[†,∥] Kanika Varshney,[†,∥] Neetu Singh,[‡] Vaibhav Mishra,[‡] Mridula Saxena,[†,§] Gautam Palit,[‡] and Anil K. Saxena*[,†]

[†]Medicinal and Process Chemistry Division and [‡]Pharmacology Division, CSIR−Central Drug Research Institute, Lucknow, 226001, India

Supporting Information

ABSTRACT: The present study revisited the three-dimensional (3D) homology model of CCK-2R using human A_{2a} adenosine receptor and the resolved NMR based structure of the third extracellular loop of the CCK-2R as templates. Further in order to identify novel antiulcer agents, rational designing have been performed utilizing the substructure of a well-known CCK-2R antagonist benzotript as a lead molecule and submitted to the combined docking and simulation studies. This led to the understanding of the essential structure requirement as well as variation of binding mode among conformational isomers of small molecule CCK-2R antagonists. In the next step, preparation of each configurational isomer of these molecules was carried out and submitted for their in vitro activity followed by in vivo screening into antiulcer rat model. The biological screening of these compounds has not only validated the developed homology model of CCK-2R but also led to the identification of highly potent CCK-2R antagonist **6a** as an orally active and safe candidate molecule having better antiulcer properties than the well-known drug benzotript.

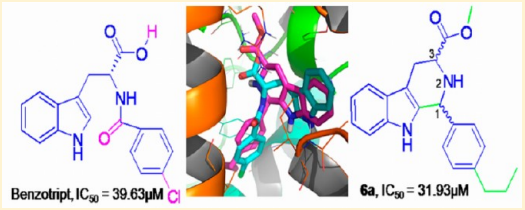

1. INTRODUCTION

The cholecystokinin (CCK) receptor plays a major role in the pathophysiology of gastrointestinal disorders such as acid reflux, gastroesphogeal reflux disease, peptic ulcers[1] as well as GI adenocarcinoma[2] and tumors.[3] The CCK-Rs belong to G-protein coupled receptor (GPCR) superfamily characterized by the presence of seven transmembrane (TM) domains separated by alternating three intracellular (N-terminal) and three extracellular (C-terminus) loop regions.[4] The CCK-Rs have been classified into two distinct classes designated as CCK-1 and CCK-2 on the basis of their affinity for the peptide agonists CCK and gastrin. Although both CCK and gastrin share an identical carboxyl-terminal pentapeptide sequence, they differs toward their selectivity for CCK-1 and CCK-2Rs.[5,6] The CCK-1Rs are specific for CCK, whereas CCK-2Rs recognize both CCK and gastrin with high affinity. The gastrointestinal polypeptide hormone gastrin has been known to stimulate gastric acid secretion and gastrointestinal cell growth in peripheral tissues. Hence, efforts have been made to develop agents that inhibit gastrin secretion, by acting through CCK-2R antagonists.[7]

Since Merck discovered asperlicin[8] as the first natural product based nonpeptide CCK-R antagonist, the quest for the drug that may block the actions of the peptide hormone gastrin has been started which led to the discovery of a wide range of small-molecule ligands.[9] Although numerous non-peptide CCK-2R antagonists have been forwarded as potential therapeutic agents for gastrointestinal disease, to date their promise remains unrealized[10] due to their unfavorable and variable biological effects.[11] Therefore, there is still a considerable interest in the development of novel small molecule CCK-2R antagonists with improved biological profile. The knowledge about the 3D structure of the target may significantly add in the understanding of essential structural requirements as well as biological activity variation among the different ligands acting on the same target. The exact cocrystallized structure of this receptor is still unknown presenting a major bottleneck for structure based discovery of novel CCK-2R antagonists and therefore earlier attempts have been made to predict its 3D structure. To date, all of the reported CCK-2R homology models have been basically derived from a homology model described by Jagerschmidt et al. built several years ago.[12] This CCK-2R model was itself obtained from an AT_{1a} receptor homology model[13] and was constructed using the transmembrane (TM) helical positions found in bacteriorhodopsin structure. This starting CCK-2R model was then successively modified to take into account new data coming from improvements of inactive bovine rhodopsin three-dimensional structures.[14,15] The major drawbacks of using bovine rhodopsin as template include the less similarity (29%) and higher gap (5%) with rat CCK-2R and the divergences among ligand binding sites. Further, in the light of resolved NMR based structure of the third extracellular loop of

Received: August 3, 2012
Published: December 16, 2012

   dx.doi.org/10.1021/ci3003655 | J. Chem. Inf. Model. 2013, 53, 176−187

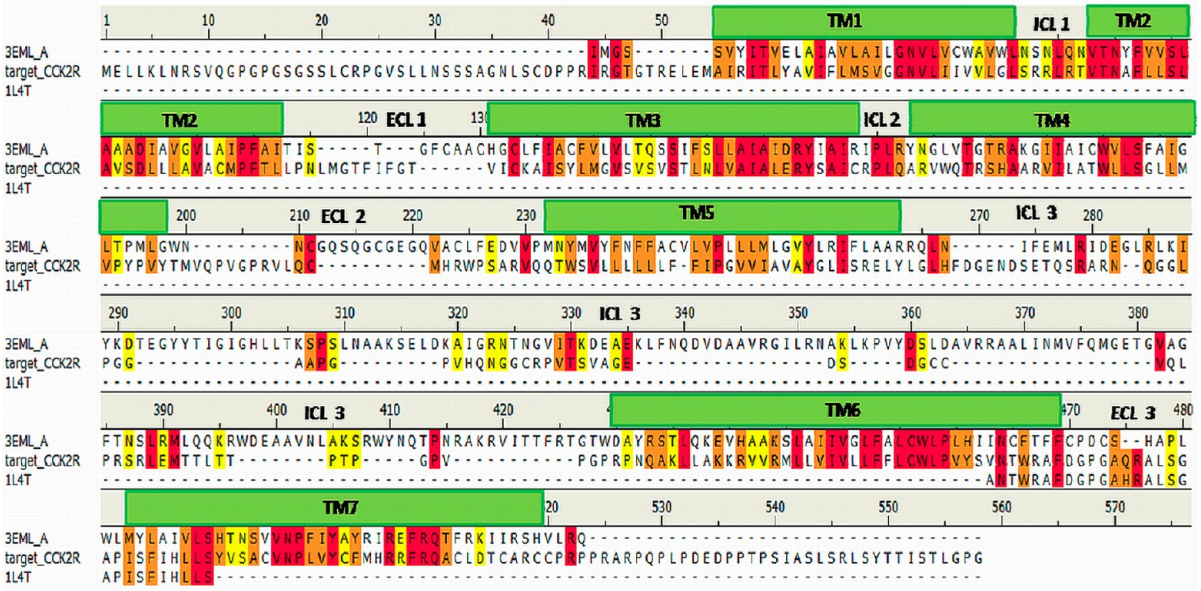

Figure 1. Multiple sequence alignment of human A_2a adenosine receptor (PDB ID 3EML) and third extracellular loop of the CCK-2R (PDB ID 1L4T) with rat CCK-2R (entry code P30553). The 7 TMs (TM1−TM7) are highlighted by green rectangles and are separated by extracellular (ECL1−3) and intracellular (ICL1−3) loops. The identical residues are shown in red color while residues with moderate and weak similar residues are shown in orange and light yellow colors.

the CCK-2R (PDB ID 1L4T),[16] there is a need to rebuild and validate the 3D structure of CCK-2R.

The present study revisited the three-dimensional (3D) homology model of CCK-2R using human A_{2a} adenosine receptor (PDB ID 3EML)[17] and the resolved NMR based structure of the third extracellular loop of the CCK-2R (PDB ID 1L4T) as templates. This is followed by the designing of molecules utilizing the substructure of well-known CCK-2R antagonist benzotript. Rigorous docking and simulation studies have been carried out to understand the essential structure requirements as well as variation of binding modes among conformational isomers of these ligands and all the configurational isomer of these molecules were prepared. The detailed biological screening of these compounds validated the plausible homology model of CCK-2R and also led to the identification of compound **6a** with better antiulcer properties than the known drug benzotript.

2. RESULT AND DISCUSSION

2.1. Generation of Preliminary Homology Model of CCK-2R. The BLAST analysis for the rat CCK-2R (Swissprot entry code P30553)[18] showed less identity (29%) and higher gap (5%) for bovine rhodopsin (PDB ID 1F88) whereas the human A_{2a} adenosine receptor (PDB ID 3EML) showed the highest identity (32%) with least gap (1%) for among the GPCRs class having PDB coordinates. This result suggests the human A_{2a} adenosine receptor as a better candidate of choice as template for rat CCK-2R. However since the third extracellular loop structure of CCK-2R has been resolved (1L4T), it showed 96% identity with rat CCK-2R and hence this loop has been also incorporated in building the homology model.

In order to find out the homology between binding sites of rat CCK-2R with other PDBs, a comparison of sequence identity and similarity was made. The global sequence identity and similarity between the rat CCK-2R and bovine rhodopsin was found as 16% and 29%, respectively, whereas the same was found as 17% and 32%, respectively, between the rat CCK-2R and the human A_{2a} adenosine receptor. However, these values further increased to 30% and 57% if only transmembrane (TM) region was considered. This analysis further projected the human A_{2a} adenosine receptor as best candidate for template selection. Therefore, in view of the drawbacks of the earlier studies as described above and in the Introduction section, a plausible homology model of the rat's CCK-2R was generated using Modeller9v9[19] considering a high-resolution crystal structure of human A_2a adenosine receptor (PDB ID 3EML) as main template and incorporating the NMR based resolved structure of the third extracellular loop of the CCK-2R (PDB ID 1L4T) as a template of this region. The amino acid sequence of the CCK-2R was retrieved from Swissprot database (entry code P30553)[18] and initially ClustalW based multiple sequence alignment was performed using these two templates using "align2d_mult" script implemented in the Modeller9v9 so that motifs common to all GPCRs and conserved amino acids between these sequences precisely matched. However, manual alignment of second template (PDB ID 1l4t) was performed to place it at the third extracellular loop of the CCK-2R. Highly conserved residues in each TM were anchored and the 10 plausible models for CCK-2R were generated using the "model-mult" script of the modeler v9.9 (Figure 1). Among the generated models, the best model was selected on the basis Ramachandran plot, low restraint violations, and low numbers of main- and sidechain bad conformations.

Though the homology model reported by us belongs to the rat family of CCK-2R utilizing the human AT_{1a} receptor, in view of 88% sequence identity between human and rat CCK-2R, a comparison of sequence alignment has been performed between the alignment reported in the present manuscript with the alignment reported by Surgand et al.[20] where the authors have described the human CCK-2R under human peptides receptor cluster and performed the alignment of 26 receptors in this category to obtain the nature of critical residues and in constructing the phylogenetic tree.[20] The alignment comparison studies showed that our alignment corresponds well with

dx.doi.org/10.1021/ci3003655 | J. Chem. Inf. Model. 2013, 53, 176−187

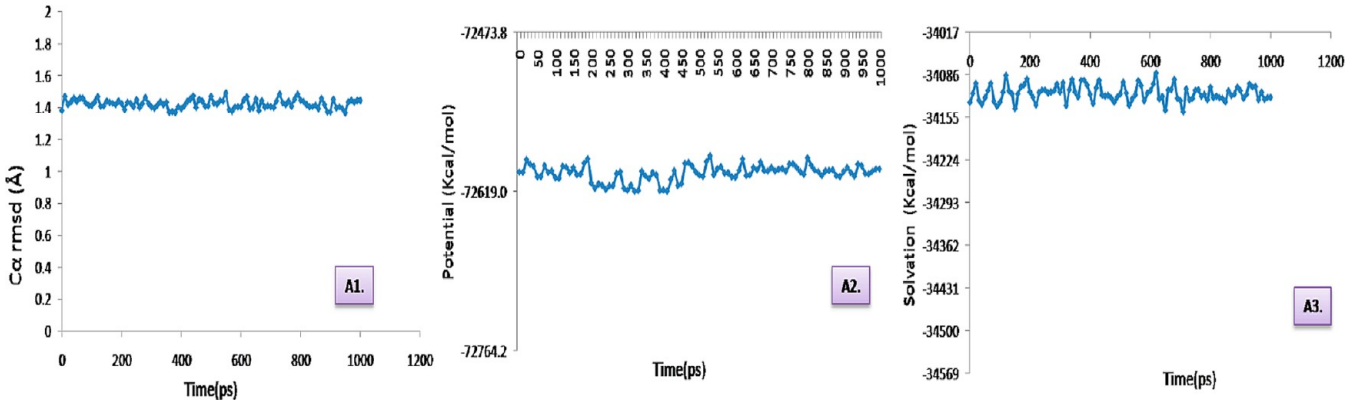

Figure 2. Graphical plot analysis of potential energy, Cα backbone rmsd, and solvation energy from 100 sampled structures of loop refined CCK-2R model.

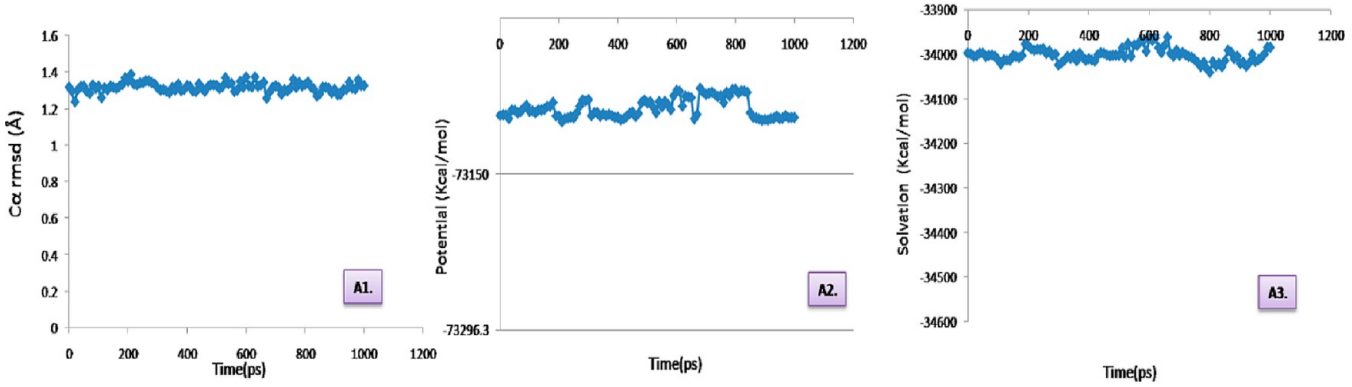

Figure 3. Graphical plot analysis of Cα backbone rmsd, potential energy, and solvation energy from 100 sampled structures of docked poses of the benzotript−CCK-2R complex.

the earlier studies where all the specified residues in the assigned TM helixes were also found in the same TM helixes. Alignment comparison in terms of highly conserved, moderately conserved, and less conserved residues was also in agreement with the earlier studies where the $F^{6.44}$ (Phe347) and $W^{6.48}$ (Trp351) residues were also found highly conserved in our study similar to the earlier study as shown in Figure 1; whereas among the moderately conserved $Y^{1.39}$ (Tyr61), $I^{1.42}$ (Ile64), and $V^{3.36}$ (Val138) residues, Ile64 was found highly conserved, Val138 was found less conserved, but Ile61 did not show any similarity in our study. Among the less conserved $C^{2.57}$ (Cys107), $M^{2.58}$ (Met108), $I^{4.56}$ (Leu185), and $W^{5.38}$ (Trp208) residues reported by Surgand et al. Cys107 was also found less conserved, and Met108 was found moderately conserved, while Leu185 and Trp218 were found highly conserved in our study.

2.2. Model Refinements. *2.2.1. Loop Refinement and Solvent Based Molecular Dynamics Simulations.* This above homology model was imported to the maestro panel of the Schrodinger software package[21] where it was examined through the Ramachandran plot, and the loops with outlier residues were refined using the "refine loops" tool with the "extended medium-serial-loop sampling" procedure of the prime module of Schrodinger software package. Further, it was backbone-constrained energy minimized through OPLS 2005 force field using MacroModel.[22] The obtained CCK-2R model was further inspected for its stability through Cα constrained low-temperature (300 K) molecular dynamics simulation (MDS) for 1000 ps where all possible translational and rotational movements of individual TM helices were taken into account using MacroModel. The graphical plot analysis of Cα backbone rmsd, potential energy, and solvation energy of 100 sampled structures of 1000 ps MDS further substantiated the stability for the developed plausible CCK-2R model (Figure 2). However, among the 100 sampled structures, the plausible CCK-2R, the model with minimum potential energy state and favorable backbone conformation, was submitted to the various online server based model quality assessments.

2.2.2. Model Quality Assessment (MQA). In view of inability of one single method to consistently and accurately predict the three-dimensional structure of a protein, the resulting CCK-2R homology model was subjected to different QA methods namely Procheck,[23] ProQ,[24] ProSA-web,[25a,b] and QMEAN.[26] On the basis of the data from various MQA methods (provided in the Supporting Information), the best homology model, with no outlier in Procheck, LGscore of 2.52 in ProQ ($\geq$2.5 for very good model), QMEAN score of 0.50 (estimated model reliability lies between 0 and 1), and Z-score (ProsaWeb) of −3.40, was selected for further studies.

2.3. Application of Modeled CCK-2R in the Substructure Based Designing of Novel CCK-2R Antagonists. The application of a homology model for new lead discovery and further lead optimization has already been established.[27] The binding domain of the amino acid derived category of CCK-R antagonists is supposed to be same as the natural ligand. Despite their low CCK-R binding, the advantage of this class of molecules includes the inhibition of opioid receptors resulting in the diminishing of ulcer pain.[28] Earlier,

dx.doi.org/10.1021/ci3003655 | J. Chem. Inf. Model. 2013, 53, 176−187

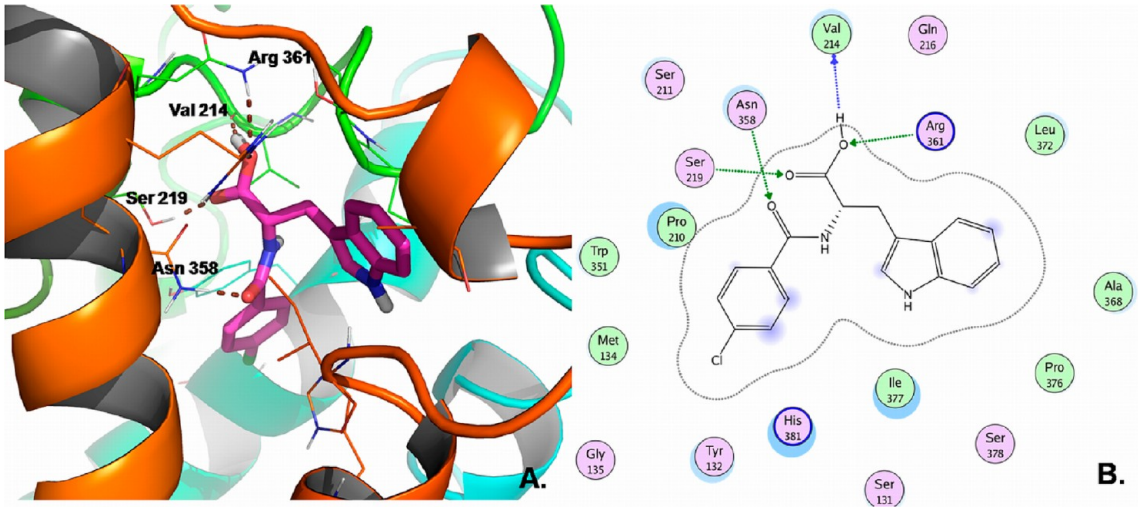

Figure 4. Binding pose analysis of benzotript at the binding site of CCK-2R. (A) Comparative 3D binding pose view of benzotript (pink color). (B) 2D binding pose view of benzotript.

the semirigid (cyclized) racemic analogues of benzotript were synthesized by our and other research groups which showed potential antiulcer activity.[29,30a,b,31a,b] Benzotript is a flexible molecule, and it may have many possible conformations. It is well known that among the many possible conformations or rotameric forms of a molecule, only a certain discrete conformation(s) are responsible for the specific biological response. Therefore to predict the biological active conformation, benzotript was submitted to the combined docking and simulation protocol. The receptor grid (active site of the protein) was generated using the residues namely His207 (EL2), Tyr189 (TM4), and Asn358 (TM6) as these residues were earlier reported to involve in the high affinity binding of the CCK to the active site of CCK-2R through site directed mutagenesis studies.[32] The structure of benzotript was drawn in the maestro panel of the Schrodinger software while the ligand preparation has been performed using the Ligprep protocol. To ensure the correct binding, the ligand protein complexes were subjected to low-temperature molecular dynamics simulation (MDS) for 1000 ps using macromodel[22] where the graphical plot analysis of Cα backbone rmsd, potential energy, and solvation energy of the protein−ligand complex of 100 sampled structures for each ligand substantiated the stability of the bound ligand into the active site of CCK-2R (Figure 3).

The binding site analysis of benzotript clearly deciphers that the hydroxylic group and ketonic oxygen of carboxylic acid showed the H bond interaction with Val214, Arg361, and Ser219, respectively. Similarly, the oxygen of benzoyl group of the molecule showed the H bond interaction with Asn358 (Figure 4A and B). The 4-chloro of the benzoyl group showed hydrophobic interactions with Tyr132, Meth134, and Trp351 while the aromatic ring itself occupied the hydrophobic cavity formed by the residues Tyr132, Trp351, and Val214. Similarly, the indole ring of the benzotript occupied the cavity made by the residues namely Pro376, Arg361, Ile377, Ala368, and Leu372 (Figure 4B).

In our continued efforts to design the novel CCK-2R antagonists with improved activity,[29,30a,b,33] the same cyclized core of benzotript was utilized to rationally design the novel CCK-2R antagonists with improved antiulcer activity (Figure 5). The chlorine atom at para position on phenyl group was substitution with propyl and methyl groups (Figure 5) as the

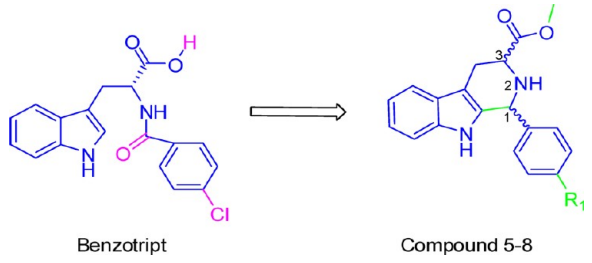

Figure 5. Substructure based approach to design compounds **5**−**8**.

incorporation of *n*-alkyl group (methyl, propyl) was considered to add more hydrophobic volume at this position. Further, the carboxylic group present at position 3 of benzotript was replaced by its methyl ester as methyl esters have shown better antiulcer properties than their corresponding acids in our earlier studies.[29]

2.4. Docking and Simulation Studies on Designed CCK-2R Antagonists. A rigorous docking and scoring studies at the same receptor grid have been performed in order to compare and predict the binding mode among the configurational isomers of these ligands with benzotript. All the reported molecules along with benzotript were drawn in the maestro panel of the Schrodinger software where the specific chirality of these molecules were assigned while the ligand preparation has been performed using the Ligprep protocol. The induced fit docking results into many binding poses among which the best docking pose was initially selected on the basis of visual inspection of important residue interaction (either of His207, Tyr189, or Asn358) with this ligand and thereafter highest docking score. To ensure the correct binding, the ligand protein complexes were subjected to low-temperature molecular dynamics simulation (MDS) for 1000 ps using macromodel[22] where the graphical plot analysis of Cα backbone rmsd, potential energy, and solvation energy of protein ligand complex of 100 sampled structures for each ligand substantiated the stability of the bound ligand into the active site of CCK-2R. The structures of rationally designed compounds along with their Glide docking score have been listed in Table 1.

The docking study showed the crucial role of Asn358 in the modulation of small molecule CCK-2R antagonists as benzotript and other active CCK-2R antagonists. The binding

dx.doi.org/10.1021/ci3003655 | J. Chem. Inf. Model. 2013, 53, 176−187

Table 1. Summary of CCK-2R Antagonist Activity of the Synthesized Compounds along with Their Glide Docking Scores

S. no.	R_1	compound name	chirality	IC_{50} (μM)	glide docking score
1	*n*-propyl	**5a**	(1*S*,3*S*)	139.70 ± 8.19	**−8.46**
2	*n*-propyl	**5b**	(1*R*,3*S*)	278.80 ± 10.45	**−6.83**
3	*n*-propyl	**6a**	(1*R*,3*R*)	31.93 ± 4.68	**−8.98**
4	*n*-propyl	**6b**	(1S, 3R)	171.00 ± 7.39	**−8.46**
5	methyl	**7a**	(1*S*,3*S*)	180.12 ± 9.60	**−8.43**
6	methyl	**7b**	(1*R*,3*S*)	267.66 ± 9.81	**−6.60**
7	methyl	**8a**	(1*R*,3*R*)	64.60 ± 8.93	**−8.68**
8	methyl	**8b**	(1*S*,3*R*)	261.12 ± 9.12	**−7.52**
9		benzotript		**39.63 ± 6.32**	**−9.29**

site analysis of each configurational isomer of these compounds revealed that the β carboline ring of these molecules occupied the same binding cavity as with the indole ring of the benzotript (Figure 6A−C).

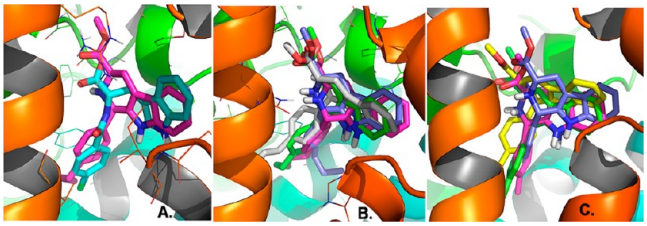

Figure 6. Comparison of binding pose view of (A) benzotript (cyan colored carbon) along with compound **6a** (pink colored carbon), (B) compound **6a** (green colored carbon), compound **6b** (pink colored carbon), **5a** (blue colored carbon), and **5b** (gray colored carbon) at the active site, (C) compound **8a** (green colored carbon), **8b** (pink colored carbon), **7a** (blue colored carbon), and **7b** (yellow colored carbon) at the active site.

More interestingly, the docking and simulation study revealed that the pendant phenyl ring attached at position 1 of the β-carboline nucleus in all of these molecules occupied the same hydrophobic cavity as with the phenyl ring of the *para*-chlorobenzoyl group of the benzotript. In order to validate the developed homology model and to identify novel CCK-2R antagonist, all four configurational isomers of each of these two molecules were prepared and evaluated for their CCK-2R antagonistic activity.

2.5. Chemistry. The synthesis of the 1,3-disubstituted tetrahydro-β-carbolines is shown in Scheme 1. Both D-(3*R*) and L-(3*S*)-tryptophan methyl esters were synthesized by our earlier reported procedure.[34] The D and L esters on Pictet−Spengler cyclizations with 4-propylbenzaldehyde and 4-methylbenzaldehyde gave the corresponding methyl 1-(4-substituted phenyl)-2,3,4,9-tetrahydo-1*H*-pyrido[3,4-b]indole-3-carboxylates as a mixture of both the cis and trans isomers as expected diastereomers. The diastereomers were separated by column chromatography using chloroform: *n*-hexane as an eluent. As the Pictet−Spengler reaction was carried out under non-stereospecific conditions, the kinetics were in support of the cis-isomer.[35] Thus, the formation of compound **5a**, **6a**, **7a**, and **8a** exceeded the formation of their counterpart trans diastereomers **5b**, **6b**, **7b**, and **8b** with % diastereomeric excess (de) of 33%, 38%, 32%, and 34%, respectively. The assignment of cis/trans stereochemistry for the tetrahydro-β-carbolines (compounds **5**−**8**) was based on a detailed study of ^{1}H and ^{13}C NMR spectroscopic data well-established in previous literature.[36] In the ^{1}H proton NMR of the cis-isomer, the H-1 signal was more upfield as compared to that of trans-isomer may be because of deshielding of H-1 in the latter by carboxylate group at the 3-position. The ^{13}C NMR signals for C-1 and C-3 were shifted more upfield in the trans isomer in relation to cis isomer with $\Delta\delta$ 3−4 ppm. This may be due to the presence of 1,3-diaxial spatial interactions in the trans isomer, where tetrahydropyridine ring exists in half-chair conformation with the ester at C-3 located equatorially. No similar difference was detected with C-3 in compounds **5**−**8**. Moreover, a 300 MHz 2D nuclear Overhauser effect spectroscopy (NOESY) experiment was done to see the correlation between the C-1 and C-3 hydrogens for *cis*-**5a** and *trans*-**5b.** The spectrum showed a clear correlation between the C-1 and C-3 hydrogens as expected for a cis relationship (figures in the Supporting Information). Mass spectrometry of all derivatives showed molecular ion peaks at $M^+ + 1$. Most of the 1,3-disubstituted-tetrahydro-β-carboline derivatives (compounds **5**−**8**) were stable as they showed the base peaks as molecular ion peaks. The infrared spectra of compounds **5**−**8** showed bands at a stretching frequency around 3400 cm^{-1} for the N−H stretching and a band around 1736 cm^{-1} for the ester carbonyl stretching. The optical rotations of derivatives (compounds **5**−**8**) showed that they are optically active, with those derived from D-tryptophan dextrorotatory and those derived from L-tryptophan levorotatory. The optical rotation angle of a 0.1% methanolic solution of derivative **5a** relative to **6a** and compound **5b** relative to **6b** showed almost equivalent values but opposite signs, indicating their enantiomeric nature. Enantiomer purity and enantiomeric excess were confirmed by chiral reverse phase high performance liquid chromatography (RP-HPLC) analysis using an alternate isocratic analytical method (Analytical Chiradex (250 mm × 4 mm, 5 μm) column, with mobile phase (60:40, ACN:MeOH) eluting at 0.5 mL/min flow rate); coinjections with each other confirmed chiral purity.

Scheme 1. Synthetic Scheme of Compounds 5−8[a]

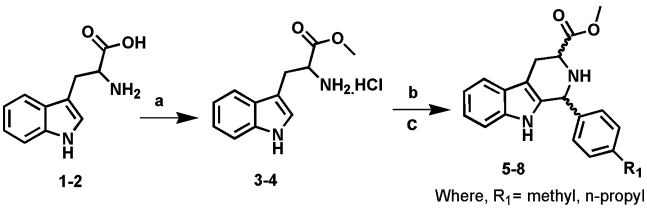

[a]Reagents and conditions (a) $SOCl_2$, MeOH, 0 °C; (b) substituted aldehydes, MeOH:H_2O, conc. HCl, 70 °C; (c) 10% Na_2CO_3.

2.6. In vitro CCK-2R Antagonist Assay. Parietal cells have been used extensively as a tool to study the antisecretory effect of any test compound in vitro. The antisecretory substances may act to inhibit gastric acid secretion by limiting the secretory responses to either histamine or gastrin. A study led by Letari et al. showed that the functional responses of gastrin on acid secretion from parietal cells can be measured by monitoring the variations in cytosolic Ca^{2+} levels as gastrin receptor/CCK-2R activation is directly coupled to cytosolic increase in Ca^{2+} ions.[37] Therefore in the present study we utilized the measurement of cytosolic Ca^{2+} decrease in gastric cells as an alternative to the functional studies for the screening of gastrin receptor/CCK-2R antagonists. The alterations in the intra-

dx.doi.org/10.1021/ci3003655 | J. Chem. Inf. Model. 2013, 53, 176−187

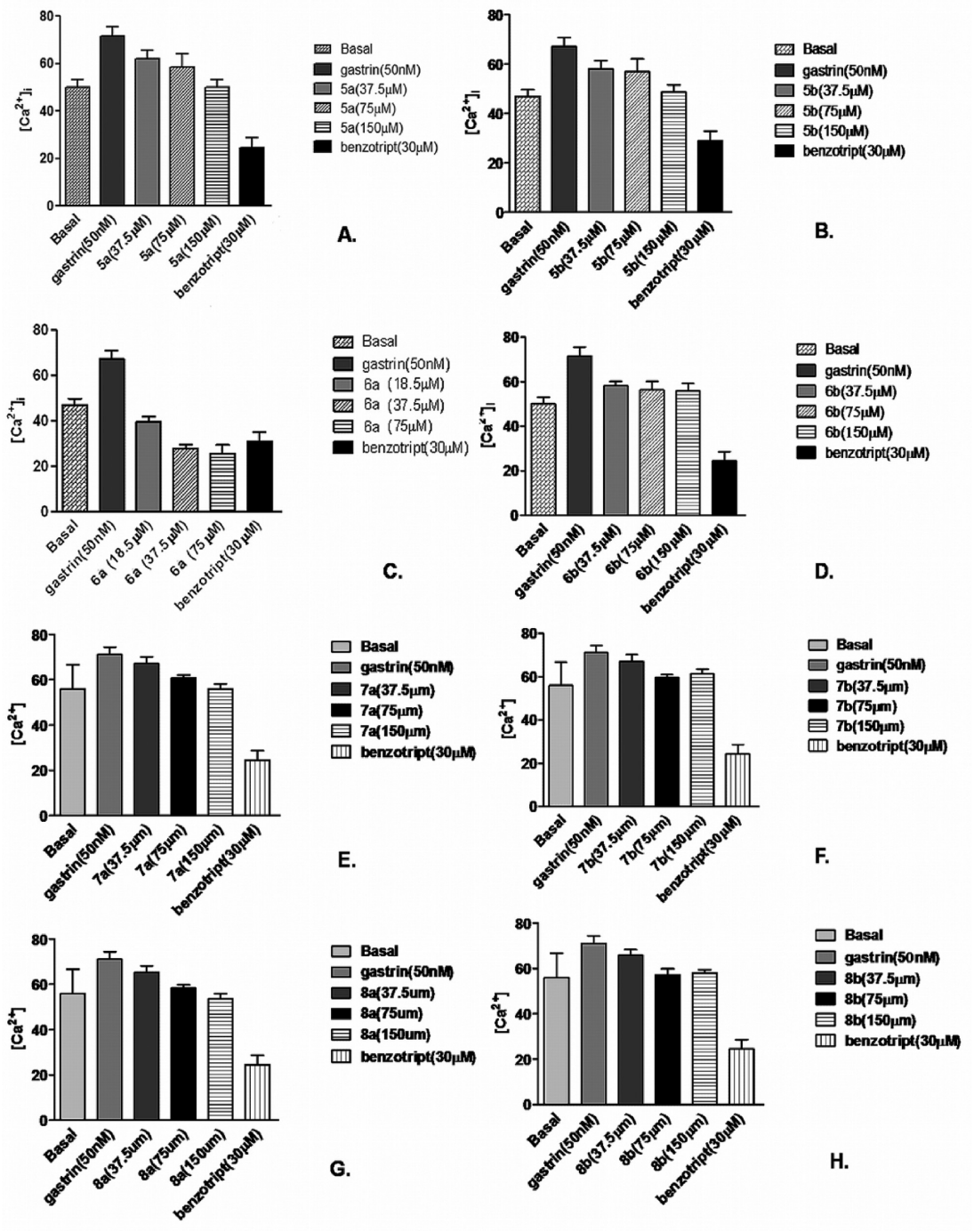

Figure 7. Dose dependent study of compounds, (A) **5a**, (B) **5b**, (C) **6a**, (D) **6b**, (E) **7a**, (F) **7b**, (G) **8a**, and (H) **8b** on intracellular $[Ca^{2+}]_i$.

cellular $[Ca^{2+}]$ ions has been examined by employing the fura-2AM method. The basal value of $[Ca^{2+}]_i$ in the resting parietal cells was (n = 3). Incubating the cells with rat gastrin (50 nM) showed an average 1.7 fold increase over basal cytosolic $[Ca^{2+}]_i$ with 67.08 ± 3.75 μM.

The dose dependent study of compound **5a** at a concentration of 37.5, 75, and 150 μM showed that it reduced the $[Ca^{2+}]_i$ with 58.2 ± 3.24, 54.9 ± 5.26, and 46.71 ± 2.96 μM, respectively (Figure 7A), resulting its IC_{50} value 139.70 μM, whereas compound **5b** at a dose of 37.5, 75, and 150 μM reduced the $[Ca^{2+}]_i$ with 62.97 ± 2.09, 55.89 ± 2.28, and 57.45 ± 1.62 μM, respectively (Figure 7B), resulting its IC_{50} value of 278.80 μM. Compound **6a** at a dose of 18.5, 37.5, and 75 μM reduced the $[Ca^{2+}]_i$ with 39.5 ± 2.33, 27.7 ± 1.67, and 25.5 ± 3.73 μM, respectively (Figure 7C), resulting its IC_{50} value 31.93 μM whereas compound **6b** at a concentration of 37.5, 75, and 150 μM reduced the $[Ca^{2+}]_i$ with 54.5 ± 1.86, 52.84 ± 3.55, and 52.41 ± 3.20 μM, respectively (Figure 7D), resulting its IC_{50} value 171.00 μM. Similarly compound **7a** at a concentration of 37.5, 75, and 150 μM reduced the $[Ca^{2+}]_i$ with 62.9 ± 3.78, 55.89 ± 1.27, and 52.45 ± 2.04 μM, respectively (Figure 7E), resulting its IC_{50} value 180.12 μM, whereas compound **7b** at a concentration of 37.5, 75, and 150 μM reduced the $[Ca^{2+}]_i$ with 62.97 ± 2.09, 55.89 ± 2.28, and 57.45 ± 1.62 μM, respectively (Figure 7F) resulting its IC_{50} value 267.66 μM. Compound **8a** at a concentration of 37.5, 75,

dx.doi.org/10.1021/ci3003655 | J. Chem. Inf. Model. 2013, 53, 176−187

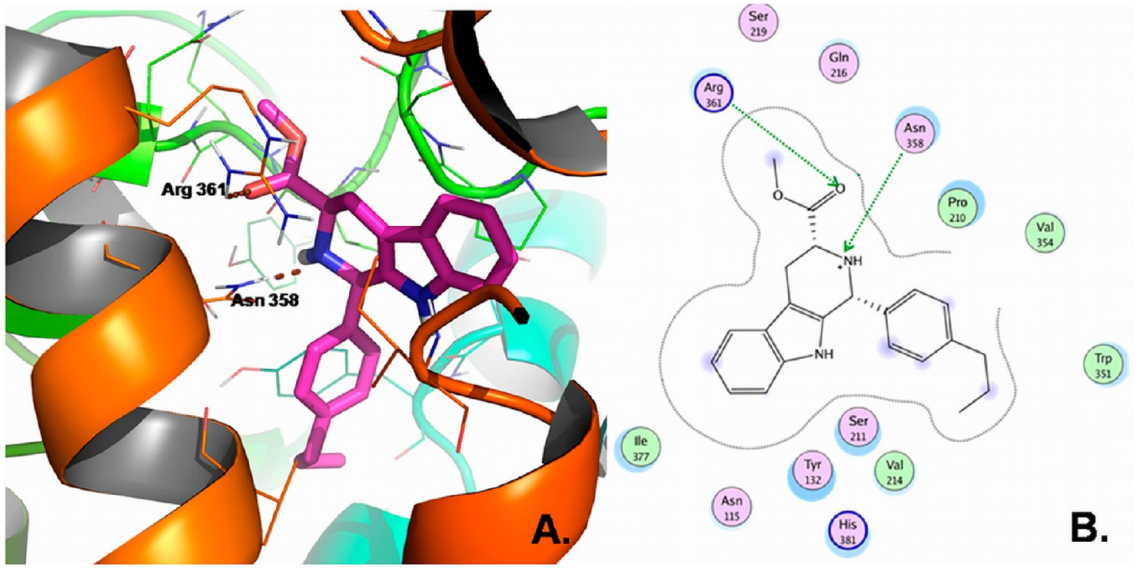

Figure 8. Binding pose analysis of compound **6a** at the binding site of CCK-2R. (A) Comparative 3D binding pose view of **6a** (pink colored carbon). (B) 2D binding pose view of **6a**.

and 150 μM reduced the $[Ca^{2+}]_i$ with 56.2 ± 2.78, 45.6 ± 1.37, and 35.2 ± 2.14, respectively (Figure 7G), resulting its IC_{50} value 63.40 μM while the compound **8b** at a concentration of 37.5, 75, and 150 μM reduced the $[Ca^{2+}]_i$ with 61.4 ± 2.39, 53.6 ± 2.58, and 54.4 ± 1.32 μM, respectively(Figure 7H), resulting its IC_{50} value 261.12 μM. Positive control used in this study as benzotript (gastrin receptor antagonist) inhibited the effect of gastrin stimulated $[Ca^{2+}]_i$ with an IC_{50} value 39.63 μM.

The above results showed that incubation of parietal cell with rat gastrin significantly elevated the intracellular Ca^{2+} level over basal values. On the basis of the dose dependent study CCK-2R antagonist activity (IC_{50}) of the eight synthesized compounds along with standard drugs benzotript has been listed in Table 1, where the gastrin augmented/CCK-2R elicited amplification of Ca^{2+} level was most significantly reversed by compound **6a**. These results suggested that compound **6a** inhibits CCK-2R more efficiently than the well-known CCK-2R antagonist benzotript. It has been observed that the docking scores were consistent with the biological activity (docking score of **5a** > **5b**, **6a** > **6b**, **7a** > **7b**, and **8a** > **8b**) where the cis isomers (1*R*,3*R* and 1*S*,3*S*) of a respective series were also more active than their corresponding trans isomers (1*S*,3*R* and 1*R*,3*S*). Further, the docking scores also corroborated with the biological activity where the compounds having *R* configuration at the C-3 position were more active than their *S* congeners at the same position. These findings were consistent with the stereoisomers having methyl (compound **8a**) or *n*-propyl group (compound **6a**) at the para position. Compound **6a** (1*R*,3*R*) having the propyl group at the *R* position and *R*,*R* configuration (cis isomer) at both the chiral center of the molecule was the most active compound. The binding site analysis comparison analysis revealed that the binding mode of compound **6a** (1*R*,3*R*) followed the similar pattern as with the benzotript (Figure 6B). However, due to formation of semirigid structure in this molecule, the Asn358 and Arg361 residues now interacts with hetrocyclic nitrogen of pyrido group and ketonic oxygen of ester group respectively through H-bonding. The para *n*-propylphenyl group of compound **6a** more accurately occupied the hydrophobic cavity (*n*-propyl group was surrounded by residues Tyr132, Met134 whereas the phenyl group was surrounded by residues Trp351 and His381, Val354, Val214, Met134, Tyr132) as compared to the *para*-chlorobenzoyl group of benzotript resulting its increased CCK2R antagonist activity over that of the benzotript (Figure 8A and B).

Compound **6b** with 1*R*,3*S* configuration had showed far reduced activity in comparison to its cis analogue **6a** (1*R*,3*R*). The docking study of compound **6b** (1*S*,3*R*) revealed that the change in the conformation of *n*-propyl phenyl group from *R* form to *S* form alter the binding site occupancy of the molecule where the *n*-propyl phenyl group now shifted toward Tyr132, but loosed its hydrophobic interaction with Trp351. Further, due to this conformation change compound **6b** also lost its H bond interaction with His361 explaining its lower antagonist activity (IC_{50}, 171.00). The binding pose analysis revealed that the n-propyl phenyl group of compound **5a** (1*S*,3*S*) showed better hydrophobic interaction with Tyr132 than the compound **6b** resulting its better CCK-2R antagonist activity than compound **6b** whereas the compound **5b** (1*R*,3*S*) which is a diastereomeric form of the molecule **5a** (1*S*,3*S*) failed to interact with any amino acid residue through H bonding resulting its least CCK-2R antagonist activity among its four possible diastereomers. The CCK-2R antagonist activity among the para methyl stereoisomers (compound **8a**, **8b**, **7a**, and **7b** of Table 1) followed the similar trend as with their *n*-propyl substituted counterpart which is also evident through the binding pose study (Figure 6C). The methyl group at para position of phenyl ring of configurational stereoisomeric compounds **8a** (1*R*,3*R*), **8b** (1*S*,3*R*), **7a** (1*S*,3*S*), and **7b** (1*R*,3*S*) interact with the hydrophobic residues, viz. Tyr 132, Met134, and Trp351, less efficiently than their respective *n*-propyl analogue resulting in the reduced activity of these compounds (Table 1)

In summary the docking study not only explained the higher activity of cis isomers (1*R*,3*R* and 1*S*,3*S*) than their corresponding trans isomers (1*S*,3*R* and 1*R*,3*S*), but it also explained the higher activity of compounds with *R* configuration at the C-3 position than their *S* congeners at the same position well.

2.7. MTT Assay. In order to evaluate the toxicity of the most active compound, the MTT assay of compound **6a** was

dx.doi.org/10.1021/ci3003655 | *J. Chem. Inf. Model.* 2013, 53, 176−187

performed on gastric cells using the protocol described by manufacturer. The relative number of viable cells/well was determined by formation of blue formazan color product by the mitochondrial dehydrogenase activity in viable cells. The treatment with the most active compound **6a** at concentrations of 5, 10, 50, and 100 μM had shown no cytotoxic effect on gastric cells (Figure 9).

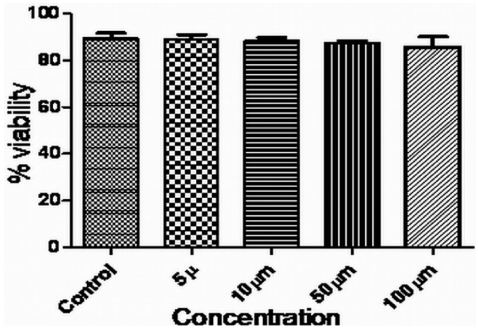

Figure 9. MTT assay of the most active compound **6a**.

2.7. In vivo Antiulcer Studies in the Cold Restraint Induced Gastric Ulcer (CRU) Model. The in vitro investigations showed that these compounds significantly inhibit the CCK-2R, and the docking study explained their biological variability. Thus, we next moved to evaluate their antiulcer/gastroprotective effect in the cold-restraint ulcer (CRU) model. Table 2 showed the in vivo percentage protection of synthesized compounds in various gastric ulcer models.

The gastric ulcer percentage protection data shown in Table 2 clearly showed that, the orally given synthetic compounds **5a**, **5b**, **6a**, **6b**, **7a**, **7b**, **8a**, and **8b** inhibited the formation of gastric ulcer in rats caused by cold and restraint stress, in a dose-related manner. Among the synthesized compounds, the most active CCK-2R antagonist, **6a**, has shown to be more efficient in reducing the gastric lesions (81.2% at a dose of 25 mg/kg, p.o.) than the reference drug benzotript (62.4% at a dose of 80 mg/kg, p.o.) in the CRU model. Cold and restraint stress alters the regulation of acid secretion by increasing the acidity of gastric juice through vagal activation.[38] Thus, the significant protection imparted by compound **6a** in this model reflected its involvement in the regulatory mechanism of gastric acid secretion.

Table 2. In vivo Percentage Protection of Synthesized Compounds in Various Gastric Ulcer Models

Compound Name	Dose mg/kg, p.o.	% ulcer protection in rat CRU model
5a	12.5	24.8
	25	43.6
	50	81.2
	100	81.0
5b	50	24.8
6a	25	81.2
6b	25	53.0
7a	25	24.8
	50	43.6
	100	43.6
7b	25	0
	50	24.8
	100	24.8
8a	25	24.8
	50	78.2
	100	81.2
8b	12.5	24.8
	25	43.6
	50	43.6
	100	43.6
Benzotript	80	62.4

3. CONCLUSION

In the past decade there has been a revived interest in CCK-2R receptor antagonists as potent anti ulcer agents due to the limitation/drawbacks of the current chemotherapies. The present study revisited the three-dimensional (3D) homology model of CCK-2R using human A_{2a} adenosine receptor and the resolved NMR based structure of the third extracellular loop of the CCK-2R as templates. In our continued efforts to design the novel antiulcer agents with improved activity, the substructure of a well-known CCK-2R antagonist benzotript has been selected as lead molecule and rational designing was performed. A combined docking and simulation study of these rationally designed molecules has led to the understanding of the essential structure requirement as well as variation of binding mode among conformational isomers of small molecule CCK-2R antagonists. In addition, the docking studies also revealed the crucial role of Asn358 for the activity of small molecule CCK-2R antagonists among three important residues involved in the interaction with CCK. In the next step, preparation of each configurationally isomer of these molecules was carried out and the compounds were submitted for their in vitro activity. The detailed in vitro and in vivo screening of these compounds has not only validated the plausible homology model of CCK-2R but also led to the identification of orally active and safe compound **6a** having better CCK-2R antagonistic and antiulcer properties than the known drug benzotript and may further be utilized for the development of potent antiulcer agent.

EXPERIMENTAL SECTION

Computational Study. All calculations were performed on a Linux workstation equipped with four parallel Intel Xeon X5460 processors (2.8 GHZ) with 12 GB total RAM.

Protein was prepared using Protein Preparation Wizard implemented in the Schrodinger package using default options: bond orders were assigned, hydrogens were added, metals were treated, and water molecules 5 Å beyond hetero groups were deleted. Hydrogens were then optimized using the exhaustive sampling option, and the protein was minimized to an rmsd limit from the starting structure of 0.3 Å using the Impref module of Impact with the OPLS_2005 force field. All ligands were drawn in the maestro panel of Schrodinger where the specific chirality of these molecules has been assigned. Further, these ligands were prepared using LigPrep protocol with Epik to expand protonation and tautomeric states at 7.0 ± 2.0 pH units.

The MDS was run using settings as OPLS-2005 as force field, water as solvent model, constant dielectric as electrostatic treatment, Polak-Ribiere Conjugate Gradient (PRCG) as minimization method, maximum iterations of 500, molecular dynamics as dynamics method, a simulation temperature of 300

dx.doi.org/10.1021/ci3003655 | J. Chem. Inf. Model. 2013, 53, 176−187

K, a time step of 1.5 fs, an equilibration time of 10 ps, and a simulations time of 1000 ps. Rest settings were used as the default in the MacroModel. The key interactions between these antagonists and the binding site residues of *CCK-2R* were presented in 3D molecular graphics, produced using the PyMol program.[39]

Chemistry. All reagents and solvents were purchased from commercial sources and used without purification. Reactions were monitored by thin layer chromatography on self-made plates of silica gel G (Merck, India) or 0.25 mm ready-made plates of silica gel 60F254, (E.Merck, Darmstadt, Germany). Column chromatography was performed on silica gel (Merck, 60 to 120 mesh). Melting points (mps) were determined on an electrical heated mp apparatus/using silicon oil bath. Infrared spectra (IR) were recorded on Perkin-FTIR model PC spectrophotometer with frequency of absorptions reported in wave numbers. MS were recorded on JEOL spectrometer with fragmentation pattern reported as values. NMR spectra were recorded with a 300 MHz spectrometers for ^{1}H NMR and 75 MHz for ^{13}C NMR on Bruker Supercon Magnet Avance DRX-300 spectrometers in deuterated solvents with TMS as internal reference (chemical shifts δ in parts per million, coupling constant J in hertz) The following abbreviations are used for multiplicity of NMR signals: s = singlet, d = doublet, q = quartet, m = multiplet, dd = doublet of doublet, br = broad. Optical rotations were measured on a Perkin-Elmer model 241 digital polarimeter. Elemental analyses were done on an Elementar Vario ELIII analyzer. Analytical Purity was assessed by chiral RP-HPLC analysis using an alternate isocratic analytical method. The stationary phase was a Analytical Chiradex (250 mm × 4.0 mm, 5 μm) column, the mobile phase employed 60:40, ACN:MeOH, and the flow rate was maintained at 0.5 mL/min.

Preparation of L-Tryptophan Methyl Ester Hydrochloride (3). Thionyl chloride (7 mL, 0.295 mol) was added dropwise to a stirred suspension of L-tryptophan **1** (10g, 0.245 mol) in dry methanol (45 mL) at −10 °C during 30 min and stirring continued for 6 h during which temperature was gradually raised from −10 °C to room temperature (25 °C). The reaction mixture was filtered under suction, and the cream colored product was washed with ether (10 mL) and dried.

Yield 58.5 g (92%). mp: 220−223 °C. $[\alpha]_D^{20}$ +17.5°. ^{1}H NMR (200 MHz, $CDCl_3$ + DMSO-d_6): δ 3.45 (d, J = 5.90, 2H), 3.75 (s, 3H), 4.17 (m, 1H), 7.07 (m, 2H), 7.28 (s, 1H), 7.41 (d, J = 7.72, 1H), 7.52 (d, J = 7.54, 1H), 8.60 (brs, 1H), 0.76 (s, 1H). FTIR (KBr cm^{-1}): 603, 731, 1034, 1225, 1285, 1352, 1443, 1499, 1580, 1748, 2021, 3292. MS(FAB): m/z 218 (M^+).

D-Tryptophan Methyl Ester Hydrochloride (4). Yield (92%). mp: 214−217 °C. $[\alpha]_D^{20}$ −17.4°. ^{1}H NMR (200 MHz, $CDCl_3$ + DMSO-d_6): δ 3.40 (d, J = 5.90, 2H), 3.72 (s, 3H), 4.14−4.21 (m, 1H), 6.98−7.13 (m, 2H), 7.39 (d, J = 7.77, 2H), 7.39 (d, J = 7.72, 1H), 7.50 (d, J = 7.52, 1H), 10.97 (brs, 1H). FTIR (KBr cm^{-1}): 3267, 1747, 1441, 1225, 1107, 1074, 731. MS(FAB): m/z 218 (M^+).

Preparation of (1*S*,3*S*) and (1*R*,3*S*)-Methyl-1-(4-propylphenyl)-2,3,4,9-tetrahydo-1*H*-pyrido[3,4-*b*]indole-3-carboxylate (5). 4-Propylbenzaldehyde (2.22 g, 15 mmol) was added to a solution of L-tryptophan methyl ester hydrochloride **2a** (2.54g, 10 mmol) in aq. methanol (22 mL; ratio 10:1) during 30 min. The reaction mixture was stirred for 4−6 h at room temperature, and progress of the reaction was monitored by TLC. Upon completion of the reaction, the reaction mixture was concentrated and cooled to give the mixture of *cis*−*trans*-(1*S*,3*S*)-methyl-1-(4-propylphenyl)-2,3,4,9-tetrahydo-1*H*-pyrido[3,4-*b*]indole-3-carboxylate which was basified with 10% aq. solution of Na_2CO_3 to give **3**. The product was extracted using ethyl acetate and the organic layer was washed with water, brine solution, and finally dried over anhydrous Na_2SO_4. It was then concentrated in vacuo to afford a residue which was purified by column chromatography (60−120 mesh) using hexane/$CHCl_3$ as eluent to seprate the respective cis isomer followed by the trans isomer.

*Cis Isomer (**5a**).* Yield 60%. mp: 90 °C. $[\alpha]_D^{20}$ −38.209° (c = 0.1, methanol). R_f = 0.78 (0.2% MeOH:CHCl3). ^{1}H NMR ($CDCl_3$, 300 MHz): δ 7.55 (s, 1H), 7.47 (s, 1H), 7.31−7.27 (m, 4H), 7.21−7.13 (m, 4H), 5.23 (s, 1H), 4.02−3.97 (dd, J_1 = 11.16 Hz, J_2 = 4.17 Hz, 1H), 3.82 (s, 3H), 3.27−3.21 (m, 1H), 2.07−2.97 (m, 1H), 2.80 (s, 1H), 2.61 (t, J = 5.30 Hz, 2H), 1.70−1.62 (m, 2H), 0.97 (t, J = 7.26 Hz, 3H). ^{13}C NMR ($CDCl_3$, 75 MHz) δ 173.09, 143.29, 137.78, 136.22, 134.65, 129.05, 128.65, 127.13, 121.90, 119.58, 118.17, 111.04, 108.72, 58.34, 56.93, 52.26, 37.81, 25.70, 24.60, 13.92. IR (KBr): 3391, 3336, 2928, 2854, 1736, 1444. MS (ESI+): m/z = 349 (M + H)$^+$. Retention time (chiral RP-HPLC): 6.45 min. Anal. calcd for $C_{22}H_{24}N_2O_2$: C, 75.83; H, 6.94; N, 8.04%. Found: C, 74.82; H, 7.05; N, 7.97%.

*Trans Isomer (**5b**).* Yield 30%. mp: 120 °C. $[\alpha]_D^{20}$ −46.111° (c = 0.1, methanol). R_f = 0.52 (0.2% MeOH:$CHCl_3$). ^{1}H NMR ($CDCl_3$, 300 MHz): δ 7.58 (s, 1H), 7.56 (s, 1H), 7.28−7.19 (m, 4H), 7.19−7.14 (m, 4H), 5.37 (s, 1H), 3.98 (t, J = 6.3 Hz, 1H), 3.73 (s, 3H), 3.27−3.21 (m, 1H), 3.32−3.25 (dd, J1 = 10.24 Hz, J2 = 5.1 Hz, 1H), 3.17−3.10 (m, 1H), 2.59 (t, J = 7.38 Hz, 2H), 1.99 (s, 1H), 1.68−1.61 (m, 2H), 0.96 (t, J = 7.26 Hz, 3H). ^{13}C NMR ($CDCl_3$, 300 MHz) δ 174.20, 142.75, 139.27, 133.51, 128.85, 128.28, 127.07, 121.91, 119.50, 118.25, 110.8, 108.42, 54.74, 52.61, 52.11, 37.74, 24.68, 24.56, 13.88; IR (KBr): 3371, 3330, 2922, 2848, 1736 1452. MS (ESI+): m/z = 349 (M + H)$^+$. Retention time (chiral HPLC): 8.20 min. Anal. calcd for $C_{22}H_{24}N_2O_2$: C, 75.83; H, 6.94; N, 8.04%. Found: C, 74.23; H, 7.15; N, 8.37%.

(1*R*,3*R*) and (1*S*,3*R*)-Methyl-1-(4-propylphenyl)-2,3,4,9-tetrahydo-1*H*-pyrido[3,4-*b*]indole-3-carboxylate (6). *Cis Isomer (**6a**).* Yield 58%. mp: 85 °C. $[\alpha]_D^{20}$ 38.209° (c = 0.1, methanol). R_f = 0.78 (0.2% MeOH:$CHCl_3$). ^{1}H NMR ($CDCl_3$, 300 MHz): δ 7.54 (s, 1H), 7.48 (s, 1H), 7.31−7.24 (m, 3H), 7.21−7.13 (m, 4H), 5.27 (s, 1H), 4.02−3.96 (dd, J_1 = 11.17 Hz, J_2 = 4.23 Hz, 1H), 3.82 (s, 3H), 3.27−3.21 (m, 1H), 2.97−3.07 (m, 1H), 2.61 (t, J = 7.35 Hz, 2H), 1.73 (bs, 1H), 1.70−1.63 (m, 2H), 0.97 (t, J = 7.29 Hz, 3H). ^{13}C NMR ($CDCl_3$, 300 MHz) δ 173.24, 143.23, 137.94, 136.13, 134.91, 129.04, 128.48, 127.17, 121.89, 119.60, 118.18, 110.92, 108.84, 58.40, 56.96, 52.21, 37.77, 25.76, 24.55, 13.85. IR (KBr): 3391, 3334, 2925, 2853, 1738 1446. MS (ESI+): m/z = 349 (M + H)$^+$. Retention time (chiral HPLC): 6.51 min. HRMS (ESI+) calcd for $C_{22}H_{24}N_2O_2$ + H: 349.1838. Found: 349.1963.

*Trans Isomer (**6b**).* Yield 26%. mp: 120 °C. $[\alpha]_D^{20}$ 46.111° (c = 0.1, methanol). R_f = 0.52 (0.2% MeOH:$CHCl_3$). ^{1}H NMR ($CDCl_3$, 300 MHz): δ 7.58 (s, 1H), 7.56 (s, 1H), 7.28−7.19 (m, 4H), 7.19−7.14 (m, 4H), 5.37 (s, 1H), 3.98 (t, J = 6.3 Hz, 1H), 3.73 (s, 3H), 3.27−3.21 (m, 1H), 3.32−3.25 (dd, J_1 = 10.24 Hz, J_2 = 5.1 Hz, 1H), 3.17−3.10 (m, 1H), 2.59 (t, J = 7.38 Hz, 2H), 1.91 (s, 1H), 1.68−1.61 (m, 2H), 0.96 (t, J = 7.26 Hz, 3H). ^{13}C NMR ($CDCl_3$, 300 MHz) δ 174.16, 142.71, 139.25, 136.16, 133.4, 128.81, 128.26, 127.03, 121.87, 119.46, 118.20, 110.88, 108.38, 54.70, 52.54, 52.07, 37.70, 24.69, 24.52,

dx.doi.org/10.1021/ci3003655 | J. Chem. Inf. Model. 2013, 53, 176−187

13.84. IR (KBr): 3371, 3330, 2922, 2848, 1736 1452. MS (ESI +): m/z = 349 $(M + H)^+$. Retention time (chiral HPLC): 7.18 min. Anal. calcd for $C_{22}H_{24}N_2O_2$: C, 75.83; H, 6.94; N, 8.04%. Found: C, 75.59; H, 7.19; N, 7.87%.

(1*S*,3*S*) and (1*R*,3*S*)-Methyl-1-(4-methylphenyl)-2,3,4,9-tetrahydo-1*H*-pyrido[3,4-b]indole-3-carboxylate (7). *Cis Isomer (**7a**).* Yield 59%. mp: 140 °C. $[\alpha]_D^{20}$ −27.0° (c = 0.1, methanol). R_f = 0.66 (0.2% MeOH:$CHCl_3$). ^{1}H NMR ($CDCl_3$, 300 MHz): δ 7.42 (d, J = 5.04 Hz, 1H), 7.29 (s, 1H), 7.24−7.00 (m, 8H), 5.12 (s, 1H), 3.89 (dd, J_1 = 10.98 Hz, J_2 = 2.91 Hz, 1H), 3.78 (s, 3H), 3.17−3.11 (m, 1H), 2.98−2.89 (m, 1H), 2.35 (s, 3H), 1.72 (s, 1H). ^{13}C NMR ($CDCl_3$, 75 MHz) δ 173.24, 138.39, 137.76, 136.16, 134.95, 129.62, 128.52, 127.18, 121.89, 119.60, 118.18, 110.93, 108.80, 58.39, 56.96, 52.21, 25.76, 21.19. IR (KBr): 3396, 3334, 2943, 2850, 1739, 1448. MS (ESI+): m/z = 321 $(M + H)^+$. Retention time (chiral HPLC): 5.45 min. Anal. calcd for $C_{20}H_{20}N_2O_2$: C, 74.98; H, 6.29; N, 8.74%. Found: C, 73.64; H, 5.90; N, 8.45%.

*Trans Isomer (**7b**).* Yield 30%. mp: 196 °C. $[\alpha]_D^{20}$ −33.034° (c = 0.1, methanol). R_f = 0.50 (0.2% MeOH:$CHCl_3$). ^{1}H NMR ($CDCl_3$, 300 MHz): δ 7.59 (s, 1H), 7.54 (d, J = 3.39 Hz, 1H), 7.25−7.14 (m, 8H), 5.35 (s, 1H), 3.95 (t, J = 3.48 Hz, 1H), 3.71 (s, 3H), 3.297−3.22 (dd, J_1 = 15.36 Hz, J_2 = 4.56 Hz, 1H), 3.15−3.07 (m, 1H), 2.34 (s, 3H), 2.04 (s,1H). ^{13}C NMR ($CDCl_3$, 75.5 MHz) δ 174.19, 139.04, 137.93, 136.19, 133.47, 129.43, 128.47, 127.03, 121.91, 119.50, 118.25, 110.95, 108.41, 54.69, 52.49, 52.15, 24.73, 21.16. IR (KBr): 3376, 3331, 2998, 2878, 1743, 1454. MS (ESI+): m/z = 321 $(M + H)^+$. Retention time (chiral HPLC): 5.87 min. Anal. calcd for $C_{20}H_{20}N_2O_2$: C, 74.98; H, 6.29; N, 8.74%. Found: C, 75.11; H, 6.27; N, 8.57%.

(1*R*,3*R*) and (1*S*,3*R*)−Methyl-1-(4-methylphenyl)-2,3,4,9-tetrahydo-1*H*-pyrido[3,4-*b*]indole-3-carboxylate (8). *Cis Isomer (**8a**).* Yield 57%. mp: 91 °C. $[\alpha]_D^{20}$ 27.0° (c = 0.1, methanol). R_f = 0.66 (0.2% MeOH:$CHCl_3$). ^{1}H NMR ($CDCl_3$, 300 MHz): δ 7.46 (d, J = 5.7 Hz, 1H), 7.32 (s, 1H), 7.24−7.05 (m, 8H), 5.16 (s, 1H), 3.95−3.89 (dd, J_1 = 11.04 Hz, J_2 = 4.20 Hz, 1H), 3.79 (s, 3H), 3.20−3.14 (dd, J_1 = 12.06 Hz, J_2 = 2.40 Hz, 1H), 3.01−2.92 (m, 1H), 2.36 (s, 3H). ^{13}C NMR ($CDCl_3$, 300 MHz) δ 173.20, 138.41, 137.68, 136.15, 134.88, 129.61, 128.51, 127.16, 121.90, 119.60, 118.18, 58.38, 56.90, 52.21, 25.72, 21.17. IR (KBr): 3396, 3333, 2941, 2849, 1740, 1448. MS (ESI+): m/z = 321 $(M + H)^+$. Retention time (chiral HPLC): 5.49 min. Anal. calcd for $C_{20}H_{20}N_2O_2$: C, 74.98; H, 6.29; N, 8.74%. Found: C, 75.04; H, 5.76; N, 8.86%.

*Trans Isomer (**8b**).* Yield: 28%. mp: 190 °C. $[\alpha]_D^{20}$ 33.034° (c = 0.1, methanol). R_f = 0.50 (0.2% MeOH:$CHCl_3$). ^{1}H NMR ($CDCl_3$, 300 MHz): δ 7.70 (s, 1H), 7.58 (m, 1H), 7.27−7.16 (m, 7H), 5.35 (s, 1H), 3.97 (t, J = 6.66 Hz, 1H), 3.73 (s, 3H), 3.32−3.25 (dd, J_1 = 15.39 Hz, J_2 = 5.22 Hz, 1H), 3.17−3.09 (dd, J_1 = 14.37 Hz, J_2 = 6.0 Hz, 1H), 2.36 (s, 3H), 2.27 (s, 1H). ^{13}C NMR ($CDCl_3$, 300 MHz) δ 174.12, 139.02, 137.89, 136.21, 133.44, 129.40, 128.34, 127.03, 121.89, 119.47, 118.21, 110.93, 108.38, 54.68, 52.47, 52.08, 24.72, 21.11. IR (KBr): 3400, 3330, 2951, 2846, 1742, 1450. MS (ESI+): m/z = 321 $(M + H)^+$. Retention time (chiral HPLC): 5.75 min. Anal. calcd for $C_{20}H_{20}N_2O_2$: C, 74.98; H, 6.29; N, 8.74%. Found: C, 74.26; H, 6.54; N, 8.51%.

Biology. *Experimental Animals.* Experimental protocols were approved by the Institutional Ethical and Usage Committee of Central Drug Research Institute, Lucknow, following the guidelines of the Committee for the Purpose of Control and Supervision of Experiments on Animals (CPCSEA). Adult Sprague−Dawley rats, weighing 130−180 g procured from National Laboratory Animal Centre, CDRI, were used in the study. Rats were housed three to four per cage, in a room with temperature regulated at 22 ± 2 °C, with a 12 h/12 h light/dark cycle (lights on 07:00 h, lights off 19:00 h). Standard chow pellets and water were given ad libitum, except during the period when food deprivation was applied.

Intracellular Ca^{2+} Monitoring. *Preparation of Isolated Parietal Cells from Rat Stomach.* Gastric cell isolation was performed as described earlier[40] with some modifications.

Ca^{2+} Measurement. Cytosolic free Ca^{2+} concentration, $[Ca^{2+}]_i$, was monitored with the fluorescent Ca^{2+} indicator fura-2.[40,41] Cells were incubated with fura-2/AM (final concentration 4 μM) for 20 min at 37 °C in Earle's medium. After loading, the cell suspension was diluted with 10 vols. of Earle's medium, centrifuged for 5 min at 200g, finally resuspended in 10 mL of Hepes-buffered saline (HBS composition in mM: NaCl 145, KC1 5, $MgCl_2$, 1, $CaCl_2$ 1, Hepes 10, glucose 10, pH 7.4) at 5−10 × 10^6 cells/mL concentration, and kept at room temperature in the dark until use. The suspension (0.8 × $l0^6$ cells/l.5 mL) was added to a glass cuvette thermostatted at 37 °C under continuous stirring. Controls received either Ca^{2+} free HBS or dimethyl sulfoxide as vehicle. Fluorescence was measured by a dual excitation fluorimetry in a fluorescence spectrophotometer (Varian, Cary Eclipse).

Wavelengths were set at 340 and 380 nm for excitation, 505 nm for emission; data points were collected at 0.2−0.4 s intervals. $[Ca^{2+}]_i$ was estimated from the ratios of 340 and 380 nm signals according to the following equation.[41]

$$[Ca^{2+}]_i = K_d \beta R - R_{min}/R_{max} - R$$

where K_d is the dissociation constant for the fura-2-Ca^{2+} complex (224 nM), $\beta = F(380)_{min}/F(380)_{max}$, R is the ratio of fluorescence at 340 over 380 nm; R_{max} and R_{min} (fluorescence ratios at saturating and zero Ca^{2+} concentration respectively) were obtained in separate experiments by adding digitonin at 50 μM followed by 2 mM EDTA and Tris and adjusted to pH 8.3.

Statistical Analysis. Statistical analysis was performed with Prism version 3.0 software using one-way analysis of variance (ANOVA) followed by Dunnett's multiple comparison test. Probabilities of less than 5% (P < 0.05) were considered significant.

Treatment Schedule. **5a**, **5b**, **6a**, **6b**, **7a**, **7b**, **8a**, **8b**, and standard gastrin receptor antagonist benzotript were prepared in 1% sodium carboxymethylcellulose (CMC) suspension and administered orally, 45 min prior to exposure to ulcerogens to the animals at a volume of 1 mL/200 g of body weight. All animals were deprived of food for 16 h before ulcerogens exposure and were divided into three groups each group comprising of six animals (n = 6).

1. Control group of animals were treated with vehicle 1% CMC.
2. Graded doses of synthetic compounds were tested against the cold restraint ulcer (CRU) model to identify the effective dose and selected for further studies in other ulcer models.
3. Experimental group was treated with standard gastrin receptor antagonist benzotript (80 mg/kg, p.o.) in the CRU model.

Antiulcer Studies in the Cold Restraint Induced Gastric Ulcer (CRU) Model. Animals were subjected to cold and

dx.doi.org/10.1021/ci3003655 | J. Chem. Inf. Model. 2013, 53, 176−187

restraint stress after 45 min of treatment with graded doses of **5a** (12.5, 25, 50, and 100 mg/kg, p.o.), **5b** (50 mg/kg,p.o.), **6a** (25 mg/kg, p.o.), **6b** (25 mg/kg, p.o.), **7a** (25, 50, and 100 mg/kg, p.o.), **7b** (25, 50 mg/kg, p.o.), **8a** (25, 50, and 100 mg/kg, p.o.), **8b** (25, 50, and 100 mg/kg, p.o.), and standard gastrin receptor antagonist benzotript (80 mg/kg, p.o.). Rats were immobilized in a restraint cages and kept at 4 °C in an environmental chamber for 2 h.[38] The animals were then sacrificed, and stomachs were observed under Magnascope for ulcers and scored.

3-(4,5-Dimethylthiazol-2-yl)-2,5-diphenyltetrazolium Bromide (MTT) Assay. In this assay, untreated and differently treated gastric cells (described in the Result and Discussion section) were seeded in a 96-well plate at a density of 4×10^4 cells per well. A 5 μL portion of MTT (5 mg/mL) was added into each well and, then, incubated for 4 h at 37 °C in the dark. After incubation, the formazon produced in the cells appeared as dark crystals in the bottom of the wells. After incubation, 100 μL of crystal dissolving solution was added in each well and incubated for 45 min to allow the complete dissolution of the formazan crystals produced. Optical density was measured in an automatic microplate reader at a test wavelength of 530 nm and reference wavelength of 690 nm to negate the effect of cell debris. The data are presented as percentage above control (untreated samples).

■ ASSOCIATED CONTENT

Ⓢ Supporting Information

Results of validation of homology model for the CCK-2R through Procheck, and ProSA-web servers, graphical plot analysis of Cα backbone rmsd, potential energy and solvation energy of protein ligand complex of 100 sampled structures of compounds **5a**, **5b**, **6a**, and **6b**, 2D binding pose view of compounds **5a**, **5b**, **6b**, **7a**, **7b**, **8a**, and **8b**, Noesy spectra for compounds **5a** and **5b**, and elemantal analysis for compounds **5**−**8**. This material is available free of charge via the Internet at http://pubs.acs.org.

■ AUTHOR INFORMATION

Corresponding Author

*Tel.: +9152226124112/ex 4386. Fax: +9152226123405. E-mail: anilsak@gmail.com.

Present Address

[§]Department of Chemistry, AMITY University, Lucknow campus, Lucknow.

Author Contributions

[∥]These authors have contributed equally to this work.

Notes

The authors declare no competing financial interest.

■ ACKNOWLEDGMENTS

The authors are thankful for financial assistance in the form of fellowships by Indian Council of Medical Research (A.K.G., N.S., and V.M.), Ministry of health (KV), and to Sophisticated Analytical Instruments Facility (SAIF), C.D.R.I., Lucknow, for providing spectroscopic data. The technical assistance of Mr. A. S. Kushwaha, Mr. Zahid Ali, and Mr. Dayanand Vishwakarma is also acknowledged. The CSIR-CDRI manuscript number allotted to this manuscript is 8373.

■ REFERENCES

(1) (a) Vakil, N. Review article: new pharmacological agents for the treatment of gastro-oesophageal reflux disease. *Aliment. Pharmacol. Ther.* **2004**, *19*, 1041−1049. (b) Lehmann, F. S.; Hildebrand, P.; Beglinger, C. New molecular targets for the treatment of peptic ulcer disease. *Drugs* **2003**, *63*, 1785−1797.

(2) (a) Reubi, J. C.; Schaer, J. C.; Waser, B. Cholecystokinin(CCK)-A and CCK-B/Gastrin receptors in human tumors. *Cancer Res.* **1997**, *57*, 1377−1386. (b) Herranz, R. Cholecystokinin antagonists: pharmacological and therapeutic potential. *Med. Res. Rev.* **2003**, *23*, 559−605.

(3) Colucci, R.; Blandizzi, C.; Tanini, M.; Vassalle, C.; Breschi, M. C.; Del Tacca, M. Gastrin promotes human colon cancer cell growth via CCK-2 receptor-mediated cyclooxygenase-2 induction and prostaglandin E2 production. *Br. J. Pharmacol.* **2005**, *144*, 338−348.

(4) Wank, S. A. Cholecystokinin receptors. *Am. J. Physiol.* **1995**, *269*, 628−646.

(5) Lee, Y. M.; Beinborn, M.; McBride, E. W.; Lu, M.; Kolakowski, L. F.; Kopin, A. S. The human brain cholecystokinin-B/gastrin receptor. cloning and characterization. *J. Biol. Chem.* **1993**, *268*, 8164−8169.

(6) Crawley, J. N.; Corwin, R. L. Biological actions of cholecystokinin. *Peptides* **1994**, *15*, 731−755.

(7) McDonald, I. M. CCK2 receptor antagonists. *Exp. Opin. Ther. Patents* **2001**, *11*, 445−462.

(8) Liesch, J. M.; Hensens, O. D.; Springer, J. P.; Chang, R. S.; Lotti, V. J. Asperlicin, a novel non-peptidal cholecystokinin antagonist from *Aspergillus alliaceus* structure elucidation. *J. Antibiot.* **1985**, *38*, 1638−1641.

(9) Berna, M. J.; Tapia, J. A.; Sancho, V.; Jensen, R. T. Progress in developing cholecystokinin (CCK)/gastrin receptor ligands that have therapeutic potential. *Curr. Opin. Pharmacol.* **2007**, *7*, 583−592.

(10) Aly, A.; Shulkes, A.; Baldwin, G. S. Gastrins, cholecystokinins and gastrointestinal cancer. *Biochim. Biophys. Acta* **2004**, *1704*, 1−10.

(11) Herranz, R. Cholecystokinin antagonists: pharmacological and therapeutic potential. *Med. Res. Rev.* **2003**, *23*, 559−605.

(12) Jagerschmidt, A.; Guillaume-Rousselet, N.; Vikland, M. L; Goudreau, N.; Maigret, B.; Roques, B. P. His381 of the rat CCKB receptor is essential for CCKB versus CCKA receptor antagonist selectivity. *Eur. J. Pharmacol.* **1996**, *296*, 97−106.

(13) Joseph, M. P.; Maigret, B.; Bonnafous, J. C.; Marie, J.; Scheraga, H. A. A computer modeling postulated mechanism for angiotensin II receptor activation. *J. Protein Chem.* **1995**, *14*, 381−398.

(14) Gales, C. L.; Poirot, M.; Tailefer, J.; Maigret, B.; Martinez, J.; Morder, L.; Escrieyt, C.; Pradayrol, L.; Fourmy, D.; Poirot, S. S. Identification of tyrosine 189 and asparagine 358 of the cholecystokinin 2 receptor in direct interaction with the crucial c-terminal amide of cholecystokinin by molecular modeling, site-directed mutagenesis, and structure/affinity studies. *Mol. Pharmacol.* **2003**, *63*, 973−982.

(15) Langer, I.; Tikhonova, I. G.; Travers, M. A.; Lahlou, E. A.; Escrieut, C.; Maigret, B.; Fourmy, D. Evidence that interspecies polymorphism in the human and rat cholecystokinin receptor-2 affects structure of the binding site for the endogenous agonist cholecystokinin. *J. Biol. Chem.* **2005**, *280*, 22198−22204.

(16) Giragossian, C.; Mierke, D. F. Intermolecular interactions between cholecystokinin-8 and the third extracellular loop of the cholecystokinin-2 receptor. *Biochemistry* **2002**, *41*, 4560−4566.

(17) Jaakola, V. P.; Griffith, M. T.; Hanson, M. A.; Cherezov, V.; Chien, E. Y.; Lane, J. R.; Ijzerman, A. P.; Stevens, R. C. The 2.6 angstrom crystal structure of a human A2A adenosine receptor bound to an antagonist. *Science* **2008**, *322*, 1211−1217.

(18) http://www.uniprot.org/uniprot/p30553 (accessed March 12, 2012.)

(19) Eswar, N.; Marti-Renom, M. A.; Webb, B.; Madhusudhan, M. S.; Eramian, D.; Shen, M.; Pieper, U.; Sali, A. *Current Protocols in Bioinformatics*; John Wiley & Sons, Inc.: Totowa, NJ, 2006; Supplement 15, pp 5.6.1−5.6.30.

(20) Surgand, J.; Rodrigo, J.; Kellenberger, E.; Rognan, D. A chemogenomic analysis of the transmembrane binding cavity of

human g-protein-coupled receptors. *Proteins: Struct., Funct., Bioinf.* **2006**, *62*, 509−538.
(21) *Schrödinger*, version 9.1; Schrodinger, LLC: New York, 2005.
(22) *MacroModel*, version 9.8; Schrödinger, LLC, New York, NY, 2010.
(23) Laskowski, R. A.; MacArthur, M. W.; Moss, D.; Thornton, J. M. PROCHECK: a program to check the stereochemical quality of protein structures. *J. Appl. Crystallogr.* **1993**, *26*, 283−291.
(24) Cristobal, S.; Zemla, A.; Fischer, D.; Rychlewski, L.; Elofsson, A. A study of quality measures for protein threading models. *BMC Bioinf.* **2001**, *2*, 5.
(25) (a) Wiederstein; Sippl, M. J. ProSA-web: interactive web service for the recognition of errors in three-dimensional structures of proteins. *Nucleic Acids Res.* **2007**, *35*, 407−410. (b) Sippl, M. J. Recognition of errors in three-dimensional structures of proteins. *Proteins* **1993**, *17*, 355−362.
(26) Benkert, P.; Schwede, T.; Tosatto, S. C. E. QMEANclust: Estimation of protein model quality by combining a composite scoring function with structural density information. *BMC Struct. Biol.* **2009**, *9*, 35.
(27) Khare, P.; Gupta, A. K.; Gajula, P. K.; Sunkari, K. Y.; Jaiswal, A. K.; Das, S.; Bajpai, P.; Chakraborty, T. K.; Dube, A.; Saxena, A. K. Identification of novel s-adenosyl-l-homocysteine hydrolase inhibitors through homology-model-based virtual screening, synthesis, and biological evaluation. *J. Chem. Inf. Model.* **2012**, *52*, 777−791.
(28) Gaudreau, P.; Lavigne, G. J.; Quirion, R. Cholecystokinin antagonists proglumide, lorglumide and benzotript, but not L-364,718, interact with brain opioid binding sites. *Neuropeptides* **1990**, *16*, 51−55.
(29) Tripathi, R. C.; Patnaik, G. K.; Saxena, A. K. Synthesis and SAR studies in 2-substituted 1,2,34 tetraghydro 9h pyrido (3,4b) indole-3-carboxylic acid: A new class of potent antiulcer agents. *Indian J. Chem.* **1989**, *28b*, 333−337.
(30) (a) Tripathi, R. C.; Saxena, A. K.; Raghubir, R. *A process for the synthesis of novel (3S)-2-substituted 1,2,3,4-tetrahydro-9H-pyrido(3,4-b) indole-3-carboxylic acids as potential anti-CCK agents*. Ind. Patent 192802, Oct. 2005. (b) Saxena, M.; Tripathi, R. C.; Saxena, A. K.; Patnaik, G. K. *A process for the synthesis of (1R3S) and (1S3R) alkyl substituted 1,2,3,4-tetrahydro-9Hpyrido(3,4-b)indole-3-carboxylate as antiulcer agents*. Ind. Patent 183332, May 2000.
(31) (a) Molino, B. F.; Darkes, P. R.; Ewing, W. R. *Tetrahydro-pyrido-indoles as cholecystokinin and gastrin antagonists*, US Patent 5162336, Nov. 1992. (b) Evans, B. E. *B carboline as cholecystokinin and gastrin antagonists*, EP 0304223 A2, Feb 1989.
(32) Langer, I.; Tikhonova, I. G.; Travers, M. A.; Lahlou, E. A.; Escrieut, C.; Maigret, B.; Fourmy, D. Evidence that interspecies polymorphism in the human and rat cholecystokinin receptor-2 affects structure of the binding site for the endogenous agonist cholecystokinin. *J. Biol. Chem.* **2005**, *280*, 22198−22204.
(33) Gupta, A. K.; Varshney, K.; Saxena, A. K. Toward the Identification of a Reliable 3D QSAR Pharmacophore Model for the CCK2 Receptor Antagonism. *J. Chem. Inf. Model.* **2012**, *52*, 1376−1390.
(34) Saxena, A. K.; Jain, P. C.; Anand, N. Agents acting on the central nervous system. 15. 2-Substituted 1,2,3,4,6,7,12,12a-octahydropyrazino [2′,1′:6,1]pyrido[3,4-b]indoles. New class of central nervous system depressants. *J. Med. Chem.* **1973**, *16*, 560−564.
(35) (a) Ungemach, F.; DiPierro, M.; Weber, R.; Cook, J. M. Stereospecific Synthesis of trans-1,3-Disubstituted-l,2,3,4-tetrahydro-*β*-carbolines. *J. Org. Chem.* **1981**, *46*, 164−168. (b) Cox, E. D.; Cook, J. M. The Pictet-Spengler condensation: a new direction for an old reaction. *Chem. Rev.* **1995**, *95*, 1797−1842. (c) Czerwinski, K.; Deng, L.; Cook, J. Mechanism driven trans stereospecificity in the Pictet-Spengler reaction. Stereospecific fomation of trans-1,2,3-trisubstituted-tetrahydro-*β*-carbolines by condensation of Nb-diphenymethyl tryptophan isopropyl esters with aldehydes. *Tetrahedron Lett.* **1992**, *48*, 4721−4724. (d) Pulka, K.; Kulis, P.; Tymecka, D.; Frankiewicz, L.; Wilczek, M.; Kozminski, M.; Misicka, A. Diastereoselective Pictete-Spengler condensation of tryptophan with R-amino aldehydes as chiral carbonyl components. *Tetrahedron Lett.* **2008**, *64*, 1506−1514.
(36) (a) Saxena, A. K.; Jain, P. C.; Anand, N.; Dua, P. R. Synthesis of 6-phenyl & 6-methyl-1,2,3,4,6,7,12,12a-octahydropyrazino-(2′,1′:6′,1)-pyrido[3,4-b]indoles. *Ind. J. Chem.* **1973**, *11*, 417−421. (b) Sandrin, J.; Soerens, D.; Cook, J. M. Carbon-13 NMR of 1,3-Disubstituted 1,2,3,4-Tetrahydro-*β*-Carbolines. *Heterocycles* **1976**, *4*, 1249−1255. (c) Ungemach, F.; Soerens, D.; Weber, R.; DiPierro, M.; Campos, O.; Mokry, P.; Cook, J. M.; Silverton, J. V. General method for the assignment of stereochemistry of 1,3-disubstituted 1,2,3,4-tetrahydro-*β*-carbolines by carbon-13 spectroscopy. *J. Am. Chem. Soc.* **1980**, *102*, 6976−6984.
(37) Letari, O.; Mennuni, L.; Revel, L.; Colombo, S.; Makovec, F. Cytosolic Ca^{2+} evaluation in rabbit parietal cells: a novel method to screen gastrin receptor antagonists. *Eur. J. Pharmacol.* **1996**, *306*, 325−333.
(38) Kitagawa, H.; Fujiwara, M.; Osumi, Y. Effects of water-immersion stress on gastric secretion and mucosal blood flow in rats. *Gastroenterology* **1979**, *77*, 298−302.
(39) *The PyMOL Molecular Graphics System*, version 1.3r1; Schrodinger, LLC: Portland, OR, 2010.
(40) Berglindh, T. Gastric glands and cells: preparation and in vitro methods. *Methods Enzymol.* **1990**, *192*, 93−107.
(41) Grynkiewicz, G.; Poenie, M.; Tsien, R. Y. A new generation of Ca2+ indicators with greatly improved fluorescence properties. *J. Biol. Chem.* **1985**, *260*, 3440−3450.